Atmos. Chem. Phys., 12, 11917–11932, 2012
www.atmos-chem-phys.net/12/11917/2012/
doi:10.5194/acp-12-11917-2012

Atmospheric Chemistry and Physics

Effects of biogenic nitrate chemistry on the NO_x lifetime in remote continental regions

E. C. Browne[1] **and R. C. Cohen**[1,2]

[1]Department of Chemistry, University of California Berkeley, Berkeley, CA, USA
[2]Department of Earth and Planetary Sciences, University of California Berkeley, Berkeley, CA, USA

Correspondence to: R. C. Cohen (rccohen@berkeley.edu)

Received: 21 June 2012 – Published in Atmos. Chem. Phys. Discuss.: 17 August 2012
Revised: 4 December 2012 – Accepted: 7 December 2012 – Published: 17 December 2012

Abstract. We present an analysis of the NO_x budget in conditions of low NO_x ($NO_x = NO + NO_2$) and high biogenic volatile organic compound (BVOC) concentrations that are characteristic of most continental boundary layers. Using a steady-state model, we show that below 500 pptv of NO_x, the NO_x lifetime is extremely sensitive to organic nitrate ($RONO_2$) formation rates. We find that even for $RONO_2$ formation values that are an order of magnitude smaller than is typical for continental conditions significant reductions in NO_x lifetime, and consequently ozone production efficiency, are caused by nitrate forming reactions. Comparison of the steady-state box model to a 3-D chemical transport model (CTM) confirms that the concepts illustrated by the simpler model are a useful approximation of predictions provided by the full CTM. This implies that the regional and global budgets of NO_x, OH, and ozone will be sensitive to assumptions regarding organic nitrate chemistry. Changes in the budgets of these species affect the representation of processes important to air quality and climate. Consequently, CTMs must include an accurate representation of organic nitrate chemistry in order to provide accurate assessments of past, present, and future air quality and climate. These findings suggest the need for further experimental constraints on the formation and fate of biogenic $RONO_2$.

1 Introduction

Nitrogen oxides enter the atmosphere as a result of bacterial processes in soils, high temperature chemistry in lightning, and combustion of fossil fuels and biomass. Current estimates are that human creation of reactive nitrogen (both oxidized and reduced nitrogen) increased by over an order of magnitude from $\sim 15\,Tg\,N\,yr^{-1}$ to $\sim 187\,Tg\,N\,yr^{-1}$ between 1860 and 2005 (Galloway et al., 2008). This increase is one of the primary causes of air pollution, contributing directly to the production of urban ozone and secondary organic aerosol (e.g., Carlton et al., 2010; Pye et al., 2010; Pinder et al., 2012; Rollins et al., 2012). The increase in NO_x also results in an increase in the global background of OH (e.g., Wild et al., 2001). This in turn affects air pollution by increasing the global background ozone concentration (e.g., Wild et al., 2001) and making it more difficult to reduce ozone in some cities (e.g., Zhang et al., 2008; Parrish et al., 2010). This increase in ozone also affects climate directly, and both NO_x and ozone affect climate indirectly by their influence on the global lifetime of CH_4 (e.g., Fuglestvedt et al., 1999; Wild et al., 2001; Derwent et al., 2008; Fry et al., 2012). Several studies have shown that the net global impact of NO_x emissions on climate forcing is highly dependent on the location and seasonal cycle of the emissions (e.g., Fuglestvedt et al., 1999; Derwent et al., 2008; Fry et al., 2012). Consequently, there has been a significant research effort to understand emissions of NO_x from different sources such as fossil fuel combustion (e.g., van der A et al., 2008; Dallmann and Harley, 2010; Jaeglé et al., 2005), lightning (e.g., van der A et al., 2008; Hudman et al., 2007; Schumann and Huntrieser, 2007), biomass burning (e.g., van der A et al., 2008; Alvarado et al., 2010; Jaeglé et al., 2005; Mebust et al., 2011; Wiedinmyer et al., 2006), and soils (e.g., van der A et al., 2008; Bertram et al., 2005; Ghude et al., 2010; Hudman et al., 2010; Jaeglé et al., 2005). In contrast, the lifetime of NO_x, knowledge of which is necessary determine concentrations from emissions, is not as well studied.

In the vicinity of emissions, the lifetime of NO_x (defined here as concentration divided by loss rate) is a steeply nonlinear function of the concentration of NO_x (Valin et al., 2011 and references therein). In the remote continental atmosphere, emissions are more uniformly distributed and NO_x concentrations vary more slowly. Textbooks suggest that the chemical lifetime of NO_x in these regions is largely set by its reaction with OH to produce HNO_3. However, several analyses have quantified the effect of isoprene nitrate formation on the NO_x budget, showing that isoprene nitrate formation is a major sink of NO_x and implying a strong effect on NO_x lifetime (e.g., Trainer et al., 1991; Horowitz et al., 2007; Ito et al., 2007; Wu et al., 2007; Paulot et al., 2012).

In this paper we investigate how changes in the formation rate of organic nitrates ($RONO_2$) affect the NO_x budget in low NO_x, high BVOC environments. Using a steady-state model we find that the instantaneous NO_x lifetime, and consequently ozone production efficiency, is extremely sensitive to $RONO_2$ production even when production rates are an order of magnitude smaller than typical for continental conditions. Calculations using the WRF-Chem model (Weather Research and Forecasting model with chemistry) (Grell et al., 2005) with detailed $RONO_2$ chemistry added to the chemical mechanism, are shown to be consistent with the conceptual model; this indicates that the steady-state model is sufficient to serve as a guide for thinking about how changes in $RONO_2$ chemistry affect NO_x.

2 Background

Daytime chemistry in the lower troposphere encompasses two chemical regimes: a low NO_x ($NO_x = NO + NO_2$) regime in which HO_x ($HO_x = OH + HO_2 + RO_2$) self-reactions (e.g., $HO_2 + RO_2$) dominate radical loss processes, and a high NO_x regime in which radicals are lost through nitric acid production. Although low NO_x chemistry has generally been synonymous with methane and carbon monoxide chemistry, recent field observations have shown that in the presence of high biogenic volatile organic compound (BVOC) concentrations, low NO_x chemistry is significantly more complex than this textbook view. Most of these recent low NO_x, high BVOC studies have focused on understanding the production and loss processes of HO_x radicals (Lelieveld et al., 2008; Stavrakou et al., 2010; Stone et al., 2011; Taraborrelli et al., 2012; Whalley et al., 2011; Mao et al., 2012). Here, we focus on understanding the nitrogen radical budget under these conditions.

Chemical loss of NO_x is generally considered to be dominated by nitric acid formation:

$$OH + NO_2 \rightarrow HNO_3 \quad \text{(R1)}$$

Close to source regions, where NO_x concentrations are high, NO_x will also be lost through the formation of peroxy nitrates:

$$RO_2 + NO_2 + M \leftrightarrow ROONO_2 + M \quad \text{(R2)}$$

It is well known that peroxy nitrates act as a NO_x reservoir; they may be transported to rural and remote locations where they will dissociate, resulting in a net source of NO_x downwind from the emissions.

Chemical NO_x loss also occurs via the formation of alkyl and multifunctional organic nitrates of the form $RONO_2$ from the minor branch of the NO and peroxy radical reaction:

$$NO + RO_2 \rightarrow RONO_2 \quad (\alpha) \quad \text{(R3a)}$$

$$NO + RO_2 \rightarrow NO_2 + RO \quad (1-\alpha) \quad \text{(R3b)}$$

Measurements of total $RONO_2$ by thermal dissociation laser induced fluorescence (Day et al., 2002) have shown that $RONO_2$ account for a substantial fraction of oxidized nitrogen ($NO_y = NO + NO_2 + NO_3 +$ total peroxy nitrates + total alkyl and multifunctional nitrates + $HNO_3 + 2{*}N_2O_5 + HONO + ...$) in urban (Rosen et al., 2004; Cleary et al., 2005; Perring et al., 2010; Farmer et al., 2011) and rural (Murphy et al., 2006; Farmer and Cohen, 2008; Day et al., 2009; Perring et al., 2009a; Beaver et al., 2012) locations as well as downwind of the continents (Perring et al., 2010).

Isoprene nitrates are thought to be a large fraction of the organic nitrates. Global modeling studies investigating the impact of isoprene-derived nitrates on NO_x and O_3 have found large sensitivities in the net global and regional budgets of O_3 and OH to assumptions about formation, lifetime, and oxidation products of isoprene-derived nitrates (e.g., Horowitz et al., 1998, 2007; von Kuhlmann et al., 2004; Fiore et al., 2005; Ito et al., 2007, 2009; Wu et al., 2007; Paulot et al., 2012). Paulot et al. (2012) used a global CTM to calculate the impact of isoprene-derived nitrates on the NO_x budget in the tropics and found that up to 70 % of the local net NO_x sink is from the formation of isoprene-derived nitrates.

Recently, simultaneous field measurements of speciated multifunctional nitrates using chemical ionization mass-spectrometry (St. Clair et al., 2010) and measurements of total $RONO_2$ by thermal dissociation laser induced fluorescence provided the first opportunity for a comparison of the total $RONO_2$ measurement in a complex chemical environment. The sum of the individual compounds was $\sim$65 % of the total $RONO_2$ when only isoprene (first and second generation) and 2-methyl-3-buten-2-ol nitrates were included, and was almost closed when all nitrogen containing masses were included. The measurements confirmed that biogenic $RONO_2$ represent the vast majority of the total in a rural environment (Beaver et al., 2012). Recent measurements from the NASA Arctic Research of the Composition of the Troposphere from Aircraft and Satellites (ARCTAS) campaign

Table 1. Reactions and rate coefficients used in the steady-state modeling of daytime chemistry.

Reaction	Rate
$CH_4 + OH \xrightarrow{O_2} CH_3O_2 + H_2O$	$1.85 \times 10^{-12}\exp(-1690/T)$[a]
$CH_3O_2 + NO \longrightarrow NO_2 + HO_2 + HCHO$	$2.8 \times 10^{-12}\exp(300/T)$[b]
$CH_3O_2 + HO_2 \longrightarrow$ products	$4.1 \times 10^{-13}\exp(750/T)$[b]
$CH_3O_2 + CH_3O_2 \longrightarrow 0.66\ HO_2 +$ products	$9.5\times 10^{-14}\exp(390/T)$[b]
$NMVOC + OH \xrightarrow{O_2} RO_2$	See Table 2
$RO_2 + NO \longrightarrow (1-\alpha)HO_2 + (1-\alpha)NO_2 + \alpha RONO_2$	$2.7 \times 10^{-12}\exp(360/T)$[c]
$RO_2 + HO_2 \longrightarrow$ products	$2.06 \times 10^{-13}\exp(1300/T)$[d]
$RO_2 + RO_2 \xrightarrow{2O_2} 1.2\ CH_3O_2 +$ products	1.4×10^{-12}[e]
$RO_2 \longrightarrow HO_2 + OH$	$4.12\times 10^{8}\exp(-7700/T)$[f]
$RO_2 + CH_3O_2 \xrightarrow{2O_2} 0.6\ CH_3O_2 + 0.6\ HO_2 +$ products	1.4×10^{-12}[e]
$CO + HO \xrightarrow{M,O_2} HO_2 + CO_2$	$k_0 = 1.5\times 10^{-13}\ (T/300)^{0.6}$ $k_\infty = 2.1 \times 10^{9}(T/300)^{6.1}$[b,*]
$CO + OH \xrightarrow{M} HOCO \xrightarrow{O_2} HO_2 + CO_2$	$k_0 = 5.9 \times 10^{-33}(T/300)^{-1.4}$ $k_\infty = 1.1 \times 10^{-12}\ (T/300)^{1.3}$[b]
$P\ (HO_x) \longrightarrow 0.8OH + 0.2HO_2$	See Table 2
$OH + O_3 \longrightarrow HO_2 + O_2$	$1.7 \times 10^{-12}\exp(-940/T)$[a]
$OH + H_2 \xrightarrow{O_2} HO_2 + H_2O$	$7.7 \times 10^{-12}\exp(-2100/T)$[a] $H_2 = 531$ ppb**
$HCHO + OH \longrightarrow HO_2 + CO_2 + H_2O$	$5.4 \times 10^{-12}\exp(135/T)$[a]
$H_2O_2 + OH \longrightarrow HO_2 + H_2O$	$2.9 \times 10^{-12}\exp(-160/T)$[a]
$HO_2 + OH \longrightarrow H_2O + O_2$	$4.8 \times 10^{-11}\exp(250/T)$[a]
$HO_2 + O_3 \longrightarrow OH + 2O_2$	$1.0 \times 10^{-14}\exp(-490/T)$[b]
$HO_2 + HO_2 \xrightarrow{M} H_2O_2 + H_2O$	$(2.1 \times 10^{-33} \times M \times \exp(920/T) +$ $3.0 \times 10^{-13}\ \exp(460/T)) \times$ $(1 + [H_2O] \times 1.4 \times 10^{-21}\ \exp(2200/T))$[b]
$HO_2 + NO \longrightarrow OH + NO_2$	$3.45 \times 10^{-12}\exp(270/T)$[a]
$NO + O_3 \longrightarrow NO_2 + O_2$	$1.4 \times 10^{-12}\exp(-1310/T)$[a]
$NO_2 + OH \xrightarrow{M} HNO_3$	$k_0 = 1.49 \times 10^{-30}(T/300)^{-1.8}\ k_\infty = 2.58 \times 10^{-11}$[g]
$NO_2 + h\nu \xrightarrow{O_2} NO + O_3$	See Table 2

[a] IUPAC Atkinson et al. (2004, 2006), [b] JPL 2011 (Sander et al., 2011), [c] MCM v3.2 (Jenkin et al., 1997; Saunders et al., 2003), [d] MCM v3.2 RO_2+HO_2 for five carbon RO_2, [e] (Jenkin et al., 1997) RO_2 reactions secondary RO_2 with β-OH, [f] Crounse et al. (2011) using MCM v3.2 RO_2+HO_2 reaction rate with a 5 carbon RO_2 to represent isoprene peroxy + HO_2, [g] Henderson et al. (2012), * Calculated using the JPL 2011 termolecular rate for chemical activation reactions, ** Novelli et al. (1999).

(Jacob et al., 2010) show that in the low NO_x, high BVOC environment of the Canadian boreal forest, $RONO_2$ account for 18 % of NO_y and often account for at least half of the instantaneous NO_x sink (Browne et al., 2012).

3 Steady-state calculations

Here, we restrict our analysis to NO_x concentrations less than 500 pptv. Discussion on the effects of $RONO_2$ chemistry at higher NO_x concentrations can be found in Farmer et al. (2011) and are reviewed by Perring et al. (2012). These low NO_x, high BVOC environments, such as boreal and tropical forests, are generally characterized by large expanses of relatively homogeneous emissions. Consequently, even while transport can be long-range, the lifetime of different species can be short relative to changes in sources and sinks. The lifetime of NO_x is the ratio of the NO_x concentration to the loss via formation of HNO_3 and $RONO_2$. Although this lifetime may be similar to, or longer than, the length of a single day or night, since the transport pathways are over uniform environments, the air parcels still have sufficient time to approach steady-state with the sources and sinks of NO_x. This does not affect the assumption of steady-state since the cycling reactions within the NO_x family are fast. Simulations with a time-dependent box model also suggest that steady-state is applicable.

Table 2. Parameters used in the daytime steady-state model. The value of the parameters (except for NMVOC + OH) are based on the mean ARCTAS measurements from less than 2 km pressure altitude and excluding data with recent anthropogenic or biomass burning influence.

Species	Value
Temperature	285 K
Photolysis rate of NO_2	$6.2 \times 10^{-3}\,s^{-1}$
CH_4	1865 ppbv
CO	130 ppbv
O_3	40 ppbv
HO_x production rate	4.1×10^6 molecules $cm^{-3}\,s^{-1}$
HCHO	1.48 ppbv
H_2O_2	2.04 ppbv
H_2O	1.18×10^4 ppm
NMVOC+OH	$2\,s^{-1}$

3.1 Daytime

Here, we use a simplified representation of daytime chemistry (Table 1) where $P(HO_x)$ represents primary HO_x production from all sources including $O(^1D) + H_2O$, photolysis of species such as H_2O_2 and HCHO, and any others. We assume that 80 % of HO_x production results in OH and the remainder in HO_2 (from HCHO photolysis). In addition to CO and CH_4 chemistry, we include a lumped VOC that reacts with OH to form a lumped peroxy radical (RO_2 in Table 1). When this lumped RO_2 species reacts with NO, it either propagates the radicals (R3b) or forms an organic nitrate (R3a). The fraction of the time that an organic nitrate is formed R3a/(R3a + R3b) is referred to as the branching ratio (α). For specific molecules, α increases with increasing carbon number, lower temperature, and higher pressure (Arey et al., 2001).

For the other RO_2 reactions, we assume that the RO_2 species behaves like a primary or secondary peroxy radical. Following the MCM protocol, the $RO_2 + RO_2$ reaction then results in 1.2 alkoxy radicals (Jenkin et al., 1997). In the model, the alkoxy radical either instantaneously isomerizes or decomposes (i.e., we ignore the reaction with O_2) to produce a peroxy radical that is lumped with CH_3O_2 (i.e., no formation of organic nitrates upon reaction with NO). The $RO_2 + CH_3O_2$ reaction follows the same assumptions resulting in 0.6 CH_3O_2 and 0.6 HO_2. The RO_2 species undergoes an isomerization reaction with products of OH and HO_2. This reduced complexity is designed to mimic the low NO_x chemistry of isoprene (e.g., Peeters et al., 2009; Peeters and Müller, 2010; Crounse et al., 2011, 2012).

For illustrative purposes, we use the mean conditions sampled during ARCTAS at low altitude and removed from recent biomass burning influence (Table 2) as inputs to the model. We run the model at specified NO concentrations until the radicals (RO_2, CH_3O_2, HO_2, OH, and NO_2) are in steady-state and then calculate the formation of $RONO_2$ and nitric acid.

Table 3. Effective α value at various NO_x concentrations. These are calculated using Eq. (A2).

α	α_{eff} 10 pptv NO_x	α_{eff} 100 pptv NO_x	α_{eff} 500 pptv NO_x
0.1 %	0.06 %	0.08 %	0.09 %
1 %	0.64 %	0.81 %	0.87 %
5 %	3.22 %	4.03 %	4.37 %
10 %	6.43 %	8.06 %	8.74 %

Values of α equal to 0 %, 0.1 %, 1 %, 5 %, and 10 % are used to illustrate a range of conditions that vary from remote conditions removed from the continents ($\alpha = 0$ % and $\alpha = 0.1$ %) to areas influenced primarily by BVOCs (e.g., monoterpenes, isoprene) with high $RONO_2$ formation ($\alpha = 5$–10 %).

It should be noted that the α value in the steady-state model is different from what has been referred to in the literature as the "effective branching ratio" (Rosen et al., 2004; Cleary et al., 2005; Perring et al., 2010; Farmer et al., 2011). The effective branching ratio refers to the average branching ratio of the entire VOC mixture (including CO, CH_4, etc) and is therefore smaller than the branching ratio of the RO_2 species. Observations suggest that the effective branching ratio for VOC mixtures for urban regions ranges from 4–7 % (Cleary et al., 2005; Farmer et al., 2011; Perring et al., 2010; Rosen et al., 2004). The effective branching ratio for the situations calculated here ranges from 0.06–8.74 % and is dependent on NO_x due to changes in the ratio of CH_3O_2 to RO_2 with NO_x (Table 3). Full details regarding the calculation of α_{eff} and discussion of how it varies with NO_x can be found in Appendix A.

3.2 Nighttime

Nighttime chemical loss of NO_x occurs via NO_3 reactions with alkenes that have organic nitrate products, heterogeneous hydrolysis of N_2O_5, and reactions of NO_3 with aldehydes. The latter two loss processes both result in the formation of HNO_3. We consider a nighttime VOC mix that consists of three VOCs: isoprene, α-pinene, and acetaldehyde.

Since there is no suitable ARCTAS data to constrain the nighttime concentrations of alkenes and aldehydes, we use output from the WRF-Chem model to guide our choice of input concentrations (Table 5). We choose a lower estimate of 400 pptv of alkenes (which we split evenly between isoprene and α-pinene) and a mid-range concentration of 2 ppbv of acetaldehyde. In this choice of isoprene and α-pinene we do not mean to imply that this is the exact speciation of the BVOCs. Rather we choose these two alkenes to act as example species since they have different reaction rates and organic nitrate yields. Varying the split between these two

Table 4. Reactions and rate coefficients used in the steady-state modeling of nighttime chemistry.

Reaction	Rate
$NO_2 + O_3 \longrightarrow NO_3$	$1.2 \times 10^{-13}\exp(-2450/T)$[a]
$NO_3 + NO_2 \xrightarrow{M} N_2O_5$	$k_0 = 2.0 \times 10^{-30}(T/300)^{-4.4}$
	$k_\infty = 1.4 \times 10^{-12}(T/300)^{-0.7}$[a]
$N_2O_5 \xrightarrow{M} NO_3 + NO_2$	$K_{eq} = 2.7 \times 10^{-27}\exp(11\,000/T)$[b]
α-pinene+$NO_3 \longrightarrow \beta_{\alpha\text{-pinene}}RONO_2 + $ products	$1.2 \times 10^{-12}\exp(490/T)$[c]
Isoprene + $NO_3 \longrightarrow \beta_{isoprene}RONO_2 + $ products	$3.15 \times 10^{-12}\exp(-450/T)$[c]
Acetaldehyde + $NO_3 \longrightarrow HNO_3 + $ products	$1.4 \times 10^{-12}\exp(-1860/T)$[c]
$N_2O_5 \xrightarrow{H_2O,surface} 2HNO_3$	See Table 5

[a] JPL 2011 (Sander et al., 2011) [b] JPL 2011 calculated from $\frac{k_{NO_3+NO_2}}{K_{eq}}$. [c] IUPAC (Atkinson et al., 2006).

Table 5. Parameters used in the nighttime steady-state model.

Species	Value
Temperature	285 K
O_3	40 ppbv
α-pinene	200 pptv
isoprene	200 pptv
acetaldehyde	2 ppbv
$\beta_{isoprene}$	0.7
$\beta_{\alpha\text{-pinene}}$	0.3
N_2O_5 hydrolysis	$\tau = 3$ or 5 h

BVOCs has no significant impact on our conclusions. We also note that although isoprene is primarily emitted during the day, it is possible to have isoprene emitted near sunset persist into the night (e.g., Brown et al., 2009).

The reaction of NO_3 with alkenes results in an NO_3-alkene adduct that either retains or releases the nitrate functionality upon reaction with other radicals. We use the parameter β to represent the fraction that retains the nitrate functionality. Recent measurements of organic $RONO_2$ yields for the reaction of biogenic VOC with NO_3 suggest that β for isoprene is $\sim$65–70 % (Rollins et al., 2009; Perring et al., 2009b), $\sim$40–45 % for β-pinene (Fry et al., 2009), and $\sim$30 % for limonene (Fry et al., 2011). Due to experimental difficulties, most chamber studies of this type are carried out under conditions where the ratio of RO_2 to HO_2 is greatly enhanced relative to the ambient atmosphere. Since the β value depends on which radical the nitrooxy peroxy radical reacts with, these organic nitrate yields are not strictly applicable to ambient measurements. We use these chamber results as a guide and assign a β value of 30 % for α-pinene, and 70 % for isoprene.

We run the model using two different lifetimes of N_2O_5 (3 h and 5 h) with respect to heterogeneous hydrolysis. Assuming a reactive uptake coefficient of 0.01, these lifetimes correspond to aerosol surface areas of approximately 144 and 87 $\mu m^2\,cm^{-3}$ for the lifetimes of 3 h and 5 h, respectively. Both these surface areas and the reactive uptake coefficient used here are likely upper limits for a remote environment. With this simplified representation of the chemistry of these VOCs and the inorganic reactions of NO_x and O_3 shown in Table 4, we calculate the loss of NO_x to HNO_3 and to $RONO_2$ by prescribing the NO_2 concentration and assuming NO_3 and N_2O_5 are in instantaneous steady-state.

4 NO_x lifetime

4.1 Daytime

We compute the lifetime of NO_x with respect to chemical loss to $RONO_2$ and nitric acid using Eq. (1):

$$\tau_{NO_x} = \frac{[NO_x]}{\text{Loss}(NO_x)} = \frac{[NO_x]}{\sum_i \alpha_i k_{RO_{2_i}+NO}[RO_{2_i}][NO] + k_{OH+NO_2}[OH][NO_2]} \quad (1)$$

For NO_x concentrations less than 500 pptv when $\alpha = 0$ %, HNO_3 formation is the sole mechanism for NO_x loss, and the NO_x lifetime is longest at low NO_x and decreases as NO_x increases (Fig. 1). This decrease is roughly proportional to 1/[OH] (not shown) which, at low NO_x concentrations, increases as NO_x concentrations increase due to an increase of OH recycling from HO_2+ NO.

As α increases, the NO_x lifetime decreases, most significantly at the lowest NO_x concentrations. At 100 pptv NO_x, for α values in the range expected in remote forested regions, $RONO_2$ production results in a NO_x lifetime of less than 8 h ($\alpha = 5$ %) and less than 5 h ($\alpha = 10$ %), compared to a NO_x lifetime of greater than one day ($\sim$27 h) for $\alpha = 0$ %. The lifetime of NO_x peaks near NO_x concentrations of $\sim$20 pptv ($\alpha = 1$ %) to $\sim$210 pptv ($\alpha = 10$ %) for α values of at least 1 % (Fig. 1). This reflects the dependence of $RONO_2$ production on RO_2 concentrations. At low NO_x concentrations, RO_2 concentrations change rapidly as a function of NO_x, resulting in the NO_x lifetime curve behaving approximately

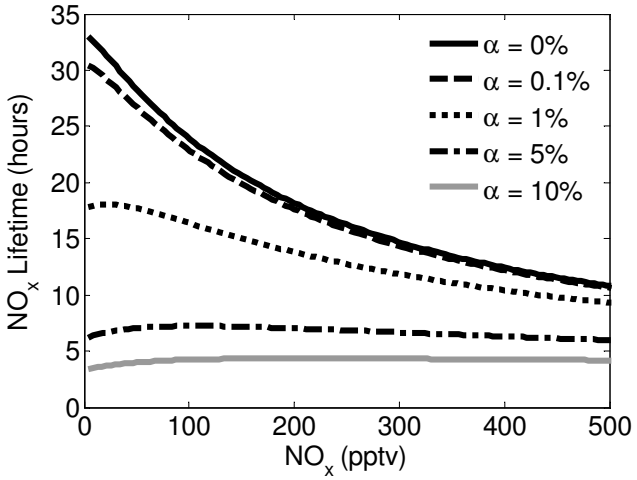

Fig. 1. Steady-state model results of NO_x lifetime to chemical loss versus NO_x concentration.

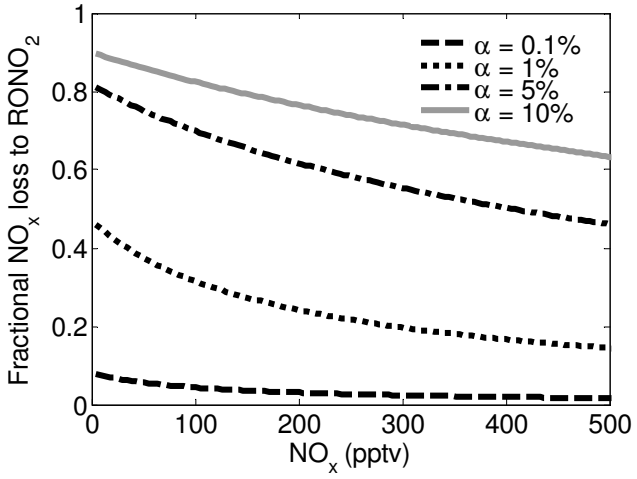

Fig. 2. Steady-state model results of fractional chemical NO_x loss to $RONO_2$ versus NO_x concentration .

as roughly proportional to $1/[RO_2]$. As NO_x increases, the change in RO_2 with NO_x slows, and the OH term becomes more important. The resulting maximum in NO_x lifetime depends on the weighting of the RO_2 term (the α value) and shifts to higher NO_x concentrations as α increases (Fig. 1).

The relative effects of HNO_3 versus $RONO_2$ formation on NO_x lifetime are shown in Fig. 2, where the fraction of NO_x loss to $RONO_2$ is shown versus NO_x. The fraction of NO_x loss to $RONO_2$ is significant at NO_x below 100 pptv-even if α is as low as 1 %. That fraction decreases as NO_x increases.

For the $\alpha = 5\,\%$ and $\alpha = 10\,\%$ cases that are expected to be typical of BVOC emissions from forests, $RONO_2$ production represents more than half of the NO_x loss at NO_x concentrations below $\sim$400 pptv and $\sim$950 pptv, respectively. Consequently, in remote regions with high BVOC emissions where we expect NO_x concentrations of $\sim$20–300 pptv, $RONO_2$ formation accounts for over 50 % of the instantaneous NO_x loss. It is notable that even for the $\alpha = 1\,\%$, which is similar to the measured value for ethane of $1.2\,\% \pm 0.2\,\%$ (Atkinson et al., 1982), $\sim$31 % of NO_x loss is due to $RONO_2$ at 100 pptv NO_x and $\sim$15 % of NO_x loss at 500 pptv NO_x. We note that the total VOC reactivity of $2\,s^{-1}$ that we use in these calculations is much too high for ethane to affect the $RONO_2$ yield ($\sim$370 ppbv of ethane are required to have a reactivity of $2\,s^{-1}$). Since the importance of $RONO_2$ decreases with decreasing VOC reactivity, we expect that $RONO_2$ formation would be low in pure ethane, CO, CH_4 chemistry. However, only $\sim$740 pptv of isoprene ($\alpha \sim 10\,\%$) is needed to achieve a reactivity of $2\,s^{-1}$ and 74 pptv of isoprene with a reactivity of $0.2\,s^{-1}$ would have the effect of $\alpha \sim 1\,\%$. Even a small addition of isoprene or other highly reactive BVOC will result in a reactivity and α in the range of these calculations.

The exact numbers presented in Figs. 1 and 2 are sensitive to the parameters chosen for HO_x production, VOC reactivity, and peroxy radical reaction rates. We have tested the effects of much slower or faster peroxy radical self reaction rates, the effect of increasing the peroxy radical isomerization rate by an order of magnitude, and the effects of varying the HO_x production and non-methane VOC reactivity. We find that the basic structure of our results, that organic nitrate formation is an important NO_x loss under low NO_x conditions, is insensitive to wide variations in the assumed parameters.

4.2 Nighttime

The nighttime formation of $RONO_2$ from NO_3 chemistry also has important implications for the chemical loss of NO_x, especially since the branching ratio for $RONO_2$ formation is much higher for NO_3 chemistry and N_2O_5 is present at very low concentrations due to low concentrations of NO_2. We calculate the NO_x lifetime at night with respect to the formation of $RONO_2$ and HNO_3 using Eq. (2) and Eq. (3) respectively.

$$\tau_{NO_x \rightarrow RONO_2} = \frac{[NO_2] + [NO_3] + 2 \cdot [N_2O_5]}{\beta_{\alpha\text{-pinene}} k_{NO_3+\alpha\text{-pinene}} [\alpha\text{-pinene}][NO_3] + \beta_{isoprene} k_{NO_3+isoprene} [Isoprene][NO_3]} \quad (2)$$

$$\tau_{NO_x \rightarrow HNO_3} = \frac{[NO_2] + [NO_3] + 2 \cdot [N_2O_5]}{2k_{N_2O_5 hydrolysis}[N_2O_5] + k_{NO_3+aldehyde}[Aldehyde][NO_3]} \quad (3)$$

For NO_x concentrations less than 500 pptv, the NO_x lifetime with respect to $RONO_2$ formation is just under 40 h and is essentially invariant with respect to assumptions regarding the N_2O_5 lifetime to hydrolysis and acetaldehyde concentrations (Fig. 3a). The lifetime shows relatively little sensitivity to reasonable changes in alkene concentration since any increase in alkenes decreases the steady-state NO_3 concentration.

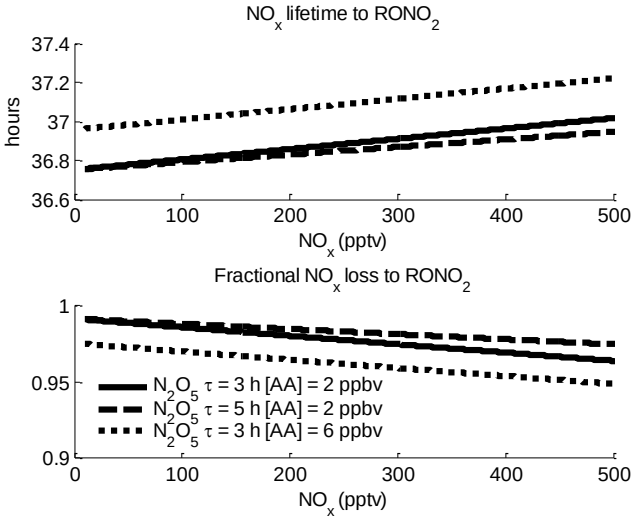

Fig. 3. Steady state model calculation of NO_x lifetime at night to **(A)** $RONO_2$ formation and **(B)** fractional NO_x loss to $RONO_2$ at night in the steady-state model.

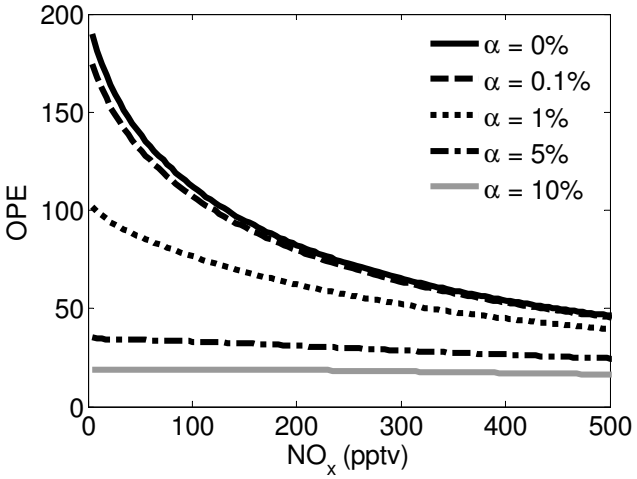

Fig. 4. Steady-state model results for ozone production efficiency (OPE) versus NO_x concentration.

The NO_x lifetime with respect to nighttime production of HNO_3 is much longer (at least several days – not shown) even for N_2O_5 hydrolysis lifetimes as short as 10 min. As a result, the fractional loss of NO_x to $RONO_2$ dominates, always accounting for at least $\sim 95\,\%$ of the fractional NO_x loss (Fig. 3b). Furthermore, increasing the HNO_3 production through the aldehyde + NO_3 reaction by increasing the acetaldehyde concentration by a factor of 3 (to 6 ppbv) results in minor differences. Even if we replace acetaldehyde with pinonaldehyde (which reacts an order of magnitude more quickly), the fraction of NO_x loss to $RONO_2$ is high: at 100 pptv NO_x it is $\sim 92\,\%$ for pinonaldehyde concentrations of 2 ppbv and 80 % for 6 ppbv pinonaldehyde (for a N_2O_5 lifetime of 180 min).

Since the lifetime is controlled by the production of $RONO_2$, the lifetime is highly sensitive to the assumed value of β; as β increases and the loss of NO_x through NO_3 reactions becomes more efficient, the NO_x lifetime will be limited by the $NO_2 + O_3$ rate. Under this condition, the NO_x lifetime is

$$\tau = \frac{[\mathrm{NO_x}]}{F k_{\mathrm{NO_2+O_3}}[\mathrm{NO_2}][\mathrm{O_3}]} \tag{4}$$

where F is a number between 1 (loss through NO_3 dominates) and 2 (loss through N_2O_5 dominates). Under low NO_x conditions F will be close to 1 and the lifetime has a limiting value at high BVOC or high β of ~ 12 h.

4.3 Twenty-four hour average lifetime

The average NO_x lifetime will be a combination of the nighttime and daytime sinks. However, the NO_x lifetime at night is much longer than the daytime value except at $\alpha = 0\,\%$ where the two are nearly equal. Under the range of NO_x concentrations studied here, the nocturnal lifetime is dominated by organic nitrate formation and is essentially invariant with NO_x concentration. Thus, the shape of the NO_x lifetime curve will be similar to the shape of the daytime lifetime curve (Fig. 1), however the curve will be shifted to longer lifetimes due to the slower loss at night.

5 Ozone production efficiency

Since the production of $RONO_2$ reduces the NO_x lifetime, it will reduce the number of ozone molecules produced per NO_x removed (the ozone production efficiency-OPE) (Fig. 4). OPE is calculated using Eq. (5):

$$\mathrm{OPE} = \frac{P(\mathrm{O_3})}{L(\mathrm{NO_x})} = \frac{k_{\mathrm{HO_2+NO}}[\mathrm{HO_2}][\mathrm{NO}] + k_{\mathrm{CH_3O_2+NO}}[\mathrm{CH_3O_2}][\mathrm{NO}] + (1-\alpha)k_{\mathrm{RO_2+NO}}[\mathrm{RO_2}][\mathrm{NO}]}{k_{\mathrm{OH+NO_2}}[\mathrm{NO_2}][\mathrm{OH}] + \alpha k_{\mathrm{RO_2+NO}}[\mathrm{RO_2}][\mathrm{NO}]} \tag{5}$$

At 100 pptv NO_x OPE decreases from ~ 110 for $\alpha = 0\,\%$ to ~ 19 for the $\alpha = 10\,\%$ case. The shape of the OPE versus NO_x curve also changes with α; the slope of the OPE versus NO_x line decreases in steepness as α increases. The shallow slope of OPE versus NO_x for the higher α cases occurs because both ozone production and NO_x loss depend on RO_2. For the low α cases, NO_x loss depends primarily on OH concentration, which, as discussed earlier, decreases as NO_x decreases. Since the RO_2 concentration increases as NO_x decreases, this results in a high OPE at low NO_x.

NO_x reservoirs, such as peroxy nitrates, transport NO_x from high NO_x, low OPE environments (urban areas) to areas downwind at lower NO_x and high OPE. Figure 4 suggests that if this downwind area is over the continents, that the OPE may be significantly lower than the traditional textbook view of low NO_x chemistry would assume. This high sensitivity

of OPE to the $RONO_2$ formation potential also suggests that small errors in $RONO_2$ representation may lead to larger errors in the calculated ozone burden.

As will be discussed further in Sect. 7, some fraction of $RONO_2$ return NO_x to the atmosphere after oxidation and consequently have a similar impact as other NO_x reservoirs such as the peroxy nitrates discussed above (with the important distinction that the NOx is returned to the atmosphere after oxidation - not just after thermal decomposition). The impact of this has been discussed by Paulot et al. (2012) who show that increases in the NO_x recycling from isoprene nitrates in the tropics increases ozone downwind of the continents. Since this is not a steady-state process, we are unable to represent using our steady-state model and instead use the 3-D chemical transport model to investigate this effect (Sect. 6). Under conditions where the return of NO_x to the atmosphere from $RONO_2$ is important, Eq. (5) should be rewritten as:

$$\mathrm{OPE} = \frac{P(\mathrm{O_3})}{L(\mathrm{NO_x})} = \frac{k_{\mathrm{HO_2+NO}}[\mathrm{HO_2}][\mathrm{NO}] + k_{\mathrm{CH_3O_2+NO}}[\mathrm{CH_3O_2}][\mathrm{NO}] + (1-\alpha)k_{\mathrm{RO_2+NO}}[\mathrm{RO_2}][\mathrm{NO}]}{k_{\mathrm{OH+NO_2}}[\mathrm{NO_2}][\mathrm{OH}] + \alpha k_{\mathrm{RO_2+NO}}[\mathrm{RO_2}][\mathrm{NO}] - \delta k_{\mathrm{RONO_2\ loss}}[\mathrm{RONO_2}]} \quad (6)$$

Here $k_{\mathrm{RONO_2\ loss}}$ represents the total effective first order loss rate of $RONO_2$ and δ refers to the fraction of this loss that returns NO_x to the atmosphere (rather than removing through processes such as deposition). It is important to note that accounting for this process simply by decreasing the α value is incorrect since the amount of NO_x returned will depend strongly on the history of the airmass and will not necessarily be representative of the local chemistry. For instance, one could imagine a forested region where there is a transition region from isoprene to monoterpene emissions. In this situation, transported isoprene nitrates may release NO_x in the monoterpene region. Due to the different properties of monoterpene nitrates and isoprene nitrates (e.g., vapor pressure, oxidation rates, deposition rates), simply decreasing the monoterpene nitrate formation will result in an inaccurate representation of the chemistry that will induce errors in calculations of ozone and SOA. Alternatively, the speciation of $RONO_2$ production may be constant, but the atmospheric conditions may change (e.g., the transition from day to night) that would result in the same species of nitrates having different integrated effects on atmospheric chemistry.

The value of OPE in the atmosphere has often been estimated using the correlation between NO_z ($NO_z = NO_y$-NO_x) and O_3, however, this is a difficult comparison due to the different lifetimes of O_3 and NO_z, as well as the variability in lifetimes of the different NO_z components. These problems are more significant in the boundary layer of remote environments where there are large contributions of peroxy nitrates and HNO_3 to NO_z. However, measurements from a forest in northern Michigan suggest an OPE of ~ 22 for NO_x concentrations around 300 pptv (Thornberry et al., 2001), an OPE value that lies between our $\alpha = 5\,\%$ and $\alpha = 10\,\%$ values expected for a forested environment.

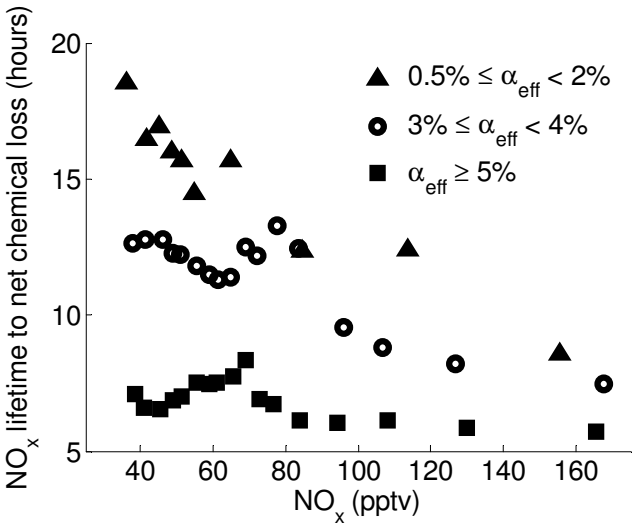

Fig. 5. WRF-Chem predication of the NO_x lifetime to net chemical loss over Canada (north of 53° N) averaged over two weeks in July. The net chemical loss is defined as the sum of the net chemical loss to different classes of NO_y including $RONO_2$, RO_2NO_2, and HNO_3 (full details can be found in Appendix B). If the net chemical loss is less than zero for any particular class, the net loss is set to zero. The results are sorted by the effective α_{eff} value as calculated using Eq. (A2).

6 Boreal forest: comparison to a 3-D chemical transport model

We compare the steady state calculations described above to the WRF-Chem 3-D chemical transport model simulations carried out using a domain that includes a large fraction of Canada where we expect low NO_x concentrations coupled with high BVOC emissions from the boreal forest to have a strong effect on NO_x lifetime. Details regarding the WRF-Chem model simulations can be found in Appendix B.

The WRF-Chem model allows us to account for the effects from NO_x reservoirs with long lifetimes relative to changes in sources and sinks (i.e. ones for which transport plays an important role in determining concentration) such as: formation and decomposition of peroxy nitrates and the release of NO_x from oxidation and photolysis of $RONO_2$. We define the NO_x lifetime with respect to the net chemical loss of NO_x. In this formulation the NO_x lifetime depends both on local chemistry as well as the decomposition of transported NO_x reservoirs. If the net chemical loss to any class of species (e.g., peroxy nitrates, $RONO_2$, nitric acid) is less than zero, then that species has zero contribution to the chemical loss of NO_x at that NO_x concentration. Figure 5 shows the NO_x lifetime to net chemical loss as a function of NO_x, binned by the effective α value calculated using Eq. (A2). In the calculation

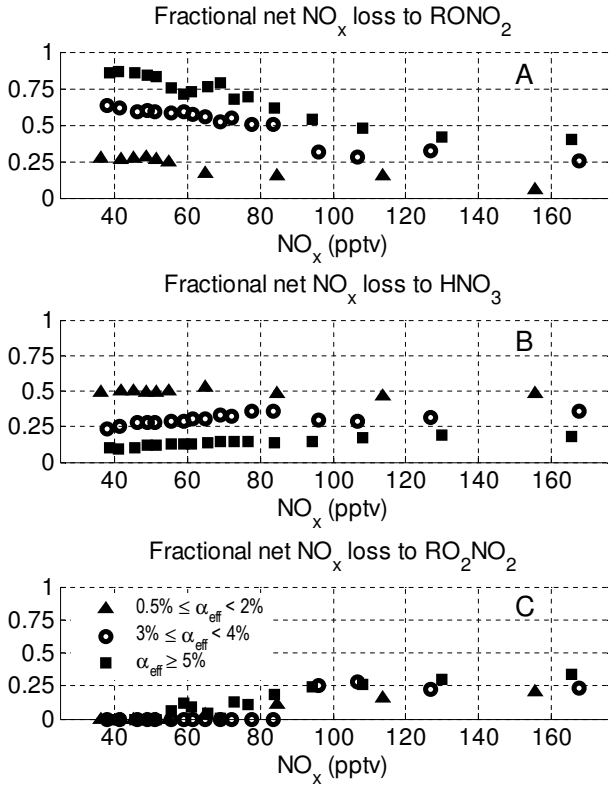

Fig. 6. WRF-Chem results for **(A)** fractional net NO_x loss to organic nitrates, **(B)** fractional net NO_x loss to HNO_3, and **(C)** fractional net NO_x loss to peroxy nitrates. The net chemical loss is defined as the sum of the net chemical loss to different classes of NO_y including organic nitrates, peroxy nitrates, and nitric acid (full details can be found in Appendix B). If the net chemical loss is less than zero for any particular class, the net loss is set to zero. The results are sorted by the effective α_{eff} value as calculated using Eq. (A2).

of α_{eff} we assume that the ozone production rate defined in Eq. (A3) is equivalent to Eq. (7):

$$P(O_3) = j_{NO_2}[NO_2] - k_{NO+O_3}[NO][O_3] \quad (7)$$

We note that the WRF-Chem results we report use 24-h averaged data to calculate α_{eff}. This allows us to sort the airmasses by their $RONO_2$ production rates; however, the exact value of α_{eff} differs slightly from what would be calculated using only the daytime data.

Within the domain, we find examples of airmasses with α_{eff} ranging from $\sim$0.4–8 %. Both the full 3-D calculations (Fig. 5) and the box model (Fig. 1) show the same general dependence of the lifetime on α: a dependence that due to the dominance of $RONO_2$ formation as a NO_x sink, is roughly proportional to $1/\alpha$. The most notable difference between the two is that the NO_x lifetime from the 3-D calculations decreases more steeply as NO_x increases than it does for the steady-state results. This is due to an increase in the loss due to peroxy nitrate formation (Fig. 6c) as NO_x increases, an effect that is not represented in the steady-state model which assumed peroxy nitrates were at steady-state and thus could be ignored.

The fractional net NO_x loss to $RONO_2$, peroxy nitrates, and HNO_3 is shown in Fig. 6. The NO_x concentrations predicted by WRF-Chem cover the range of $\sim$30–250 pptv. Although this range represents a small fraction of the global variation of NO_x concentrations, it is a typical range for the majority of remote continental regions. However, the chemistry in this regime is highly sensitive to the NO_x concentration and, as shown in both Fig. 2 for the steady state model and in Fig. 6 for the WRF-Chem model, large changes in the fractional composition of the products of the NO_x loss reactions are predicted. In both calculations the fraction of net NO_x loss to $RONO_2$ (Fig. 6a) approaches unity as NO_x decreases and as the effective α value increases. Interestingly, the WRF-Chem predictions for the fractional net NO_x loss to HNO_3 shows only a slight increase as a function of NO_x (Fig. 6b) and the decrease in fractional NO_x loss to $RONO_2$ is compensated by an increase in the net NO_x loss to peroxy nitrates when NO_x is greater than $\sim$50–80 pptv (Fig. 6c). We note that a plot of the fractional instantaneous gross loss when only $RONO_2$ and HNO_3 are considered (which is a direct comparison to Fig. 2), does show the fractional contribution of HNO_3 increasing with increasing NO_x (not shown). The fractional net NO_x loss to peroxy nitrates exhibits little variation with respect to α_{eff}, indicating that peroxy nitrates are acting to buffer NO_x. A full investigation of this effect, however, would require a larger NO_x range and attention to the effects of temperature and transport. Many of these aspects of peroxy nitrate chemistry have been discussed previously (Sillman and Samson, 1995). We note that due to the thermal instability of peroxy nitrates, the importance of peroxy nitrates as a NO_x reservoir will be highly dependent on temperature and we expect large differences between seasons and between boreal and tropical forests. In no regime does peroxy nitrate chemistry change the conclusion that the lifetime of NO_x is controlled by $RONO_2$ production rates at low NO_x concentrations.

7 Discussion

In the past few years it has become increasingly apparent that our understanding of atmospheric chemistry in low NO_x, high BVOC environments is limited. Most of the work in this chemical regime (e.g., Lelieveld et al., 2008; Peeters and Müller, 2010; Stavrakou et al., 2010; Stone et al., 2011; Taraborrelli et al., 2012; Whalley et al., 2011), however, has focused on the HO_x budget with little to no discussion on other controlling factors, including the nitrogen budget. Uncertainties in the HO_x budget, particularly regarding the fate of RO_2 and the production of OH, impact the NO_x budget via the changes in the concentrations of RO_2, HO_2, and OH which, in turn, change the absolute values of $RONO_2$ and HNO_3 production. However, the work presented here shows

that in these low NO_x, high BVOC environments the fate of NO_x also has important consequences on atmospheric chemistry. In particular we show that the formation of $RONO_2$ accounts for the majority of the instantaneous NO_x sink, resulting in decreased NO_x lifetime and decreased OPE relative to chemistry dominated by CO and CH_4. Thus, it is clear that although there are significant uncertainties associated with this chemical regime, it is necessary to consider both the HO_x and NO_x budgets.

One of the most important uncertainties regarding the impact of $RONO_2$ chemistry on regional and global scales is the extent to which these molecules serve as permanent versus temporary NO_x sinks; a value which, in general, is not well known. For instance, if we assume that $RONO_2$ predominately serve as temporary NO_x sinks that transport NO_x to areas with higher OPE (e.g., areas with lower NO_x or areas at the same NO_x but lower α), we expect an increase in the ozone burden as a result of accounting for $RONO_2$ chemistry. In contrast, if the $RONO_2$ are lost primarily through deposition, they may increase nitrogen availability in the biosphere. Since many areas are nitrogen limited, introduction of nitrogen will also affect the carbon storage capacity of an ecosystem (e.g., Holland et al., 1997; Thornton et al., 2007, 2009; Bonan and Levis, 2010). A recent study observed the direct foliar uptake of $RONO_2$ and subsequent incorporation of the nitrogen into amino acids (Lockwood et al., 2008), indicating that (at least some) $RONO_2$ will affect plant growth.

In order to improve our understanding of the impact of $RONO_2$ on atmospheric chemistry, particularly on the global and regional NO_x and HO_x budgets, laboratory studies on the formation of $RONO_2$ (particularly for biogenic species other than isoprene), oxidation, physical loss, and oxidation products are necessary. Of particular importance is improving the constraints on the extent to which organic nitrates act as permanent versus temporary sink of NO_x. This requires measurement of: the oxidation rates and products, dry and wet deposition velocities, and secondary organic aerosol formation and processing for various biogenic organic nitrates. These laboratory measurements must be supplemented by field measurements spanning NO_x concentrations from near zero to a few ppbv. In one such analysis, we use measurements from the ARCTAS campaign (Browne et al., 2012). However, a thorough understanding will require measurements in environments with different classes of BVOC emissions (e.g., pine forests which are dominated by monoterpenes ($\alpha \sim 18\,\%$) and oak forests which are dominated by isoprene ($\alpha \sim 10\,\%$)). These field measurements will provide constraints on how the importance of $RONO_2$ versus nitric acid changes as a function of NO_x and will test the representation of $RONO_2$ chemistry in condensed chemical mechanisms.

It is interesting to consider how incorporation of improved $RONO_2$ chemistry into condensed chemical mechanisms may impact our understanding of both preindustrial and future climates. For instance, it is likely that during the preindustrial era when NO_x concentrations were lower, that $RONO_2$ formation was a more important NO_x sink than it is today. Model predictions of preindustrial climate often predict larger ozone concentrations than the semi-quantitative measurements of the late 19th/early 20th century indicate (e.g., Mickley et al., 2001; Archibald et al., 2011). Although there may be problems with the ozone measurements or with the emissions estimates used in the models, this may also indicate that models are missing a NO_x sink in the preindustrial era. As shown in Fig. 4, we calculate that the OPE is very sensitive to the assumed branching ratio, indicating that a small error in $RONO_2$ formation may have a large effect on the ozone burden.

In industrialized countries, NO_x emissions are currently decreasing due to air quality control measures (e.g., van der A et al., 2008; Dallmann and Harley, 2010; Russell et al., 2010, 2012). Coupling this decrease in NO_x with the increase in biogenic VOC emissions expected in a warmer climate, suggests that $RONO_2$ chemistry will begin to play a more important role in NO_x termination in urban and suburban areas. As discussed in Sect. 4.1, the crossover from $RONO_2$ to nitric acid accounting for over 50 % of NO_x loss occurs at $\sim$400 pptv for a 5 % branching ratio and at $\sim$950 pptv for a 10 % branching ratio. Past studies have constrained the effective branching ratio in urban areas at 4–7 % (Cleary et al., 2005; Farmer et al., 2011; Perring et al., 2010; Rosen et al., 2004), which suggests that to predict ozone in future climates, it will be necessary to correctly simulate $RONO_2$ chemistry in order to understand regional pollution and air quality.

8 Conclusions

Recent field measurements have indicated that low NO_x, high BVOC chemistry is significantly more complex than the textbook view of low NO_x chemistry being controlled by methane and carbon monoxide. Most of the work on low NO_x, high BVOC chemistry has focused on the implications for the HO_x budget. In this paper we analyze how the NO_x lifetime responds to changes in $RONO_2$ production under these conditions. We find that production of $RONO_2$ accounts for the majority of the instantaneous NO_x sink in low NO_x, high BVOC environments in both a steady-state model and a 3-D chemical transport model. Furthermore, the NO_x lifetime and OPE are highly sensitive to $RONO_2$ production. These findings suggest that proper representation of $RONO_2$ formation and NO_x recycling are necessary for accurate calculation of past, present, and future ozone concentrations and the corresponding climate effects.

Appendix A

Effective branching ratio

The effective branching ratio is a measure of the average branching ratio for the VOC composition contributing to ozone production. For the steady state model, we calculate the effective α value using Eq. (A1):

$$\alpha_{\text{eff}} = \frac{\alpha k_{\text{RO}_2+\text{NO}}[\text{RO}_2]}{k_{\text{CH}_3\text{O}_2+\text{NO}}[\text{CH}_3\text{O}_2] + k_{\text{RO}_2+\text{NO}}[\text{RO}_2]} \quad \text{(A1)}$$

Here RO_2 refers to the lumped peroxy radical from Table 1. This is equivalent to

$$\alpha_{\text{eff}} = \frac{P(\text{RONO}_2)}{P(\text{O}_3) + P(\text{RONO}_2) - k_{\text{HO}_2+\text{NO}}[\text{HO}_2][\text{NO}]} \quad \text{(A2)}$$

where

$$P(\text{O}_3) = k_{\text{HO}_2+\text{NO}}[\text{HO}_2][\text{NO}] + \sum_i (1-\alpha_i) k_{\text{RO}_{2_i}+\text{NO}}[\text{RO}_{2_i}][\text{NO}]$$

$$+ k_{\text{CH}_3\text{O}_2+\text{NO}}[\text{CH}_3\text{O}_2][\text{NO}] \quad \text{(A3)}$$

$$P(\text{RONO}_2) = \sum_i \alpha_i k_{\text{RO}_{2_i}+\text{NO}}[\text{RO}_{2_i}][\text{NO}] \quad \text{(A4)}$$

Here we have generalized the production of O_3 and $RONO_2$ to account for situations of multiple peroxy radicals with an $RONO_2$ formation channel.

Unlike α, α_{eff} changes as a function of NO_x due to the dependence of α_{eff} on the ratio of RO_2 to CH_3O_2. This ratio decreases as NO_x decreases because $RO_2 + RO_2$ reactions which form CH_3O_2, the loss of RO_{2b} by isomerization, and the importance of $RO_2 + HO_2$ reactions (which are faster for RO_2 than for CH_3O_2) all increase in importance at low NO_x. As a result, α_{eff} decreases as NO_x decreases. This decrease is steepest under low NO_x conditions where, due to the high RO_2 concentrations, $RO_2 + RO_2$ reactions are most important. As shown in Table 3, the increase in α_{eff} from 10 pptv to 100 pptv ($\sim$ 20–25 % increases) is about twice the increase from 100 pptv to 500 pptv NO_x ($\sim$ 8–12 % increase).

This definition of effective branching ratio differs slightly from that used by elsewhere in the literature (Rosen et al., 2004; Cleary et al., 2005; Perring et al., 2010; Farmer et al., 2011) where the effective branching ratio is approximated as

$$\alpha_{\text{eff}} \approx \frac{2}{P(\text{O}_3)/P(\text{RONO}_2)} \approx \frac{2}{\Delta[\text{O}_x]/\Delta[\Sigma\text{ANs}]} \quad \text{(A5)}$$

where $P(O_3)$ and $P(RONO_2)$ refer to the production rate of ozone and $RONO_2$ respectively. The second equality using concentrations holds under conditions where loss rates are small. This derivation relies on the assumption that HO_2 and RO_2 radicals are present in near equal concentrations (i.e., that each RO generates a carbonyl and an HO_2) and is equal to Eq. (A2) when this assumption is valid. This assumption is appropriate under high NO_x conditions where this derivation has been used previously, but is invalid under low NO_x conditions where RO_2 concentrations are larger than HO_2 concentrations.

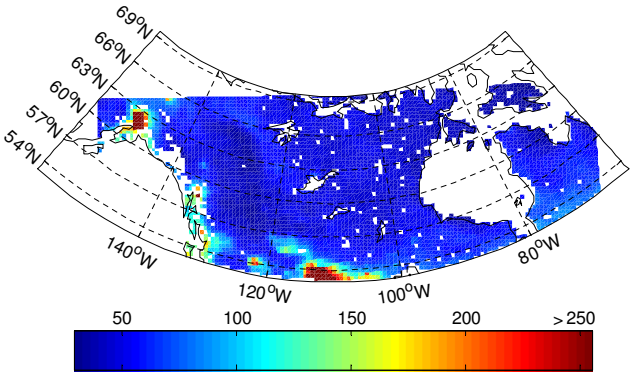

Fig. B1. NO_x (=NO+NO_2+NO_3+2*N_2O_5) concentration (pptv) over the WRF-Chem domain. This concentration represents the boundary layer average over two weeks of simulation.

Appendix B

WRF-Chem details

B1 Domain

We run the WRF-Chem model at 36 km $\times$ 36 km resolution with 29 vertical layers for 23 June–13 July 2008 using meteorological data from NARR (North American Regional Reanalysis). Biogenic emissions are from MEGAN (Guenther et al., 2006, available at http://www.acd.ucar.edu/wrf-chem/) and anthropogenic emissions are from RETRO and EDGAR using the global emissions preprocessor for WRF-Chem (Freitas et al., 2011). Boundary conditions come from the MOZART model (Emmons et al., 2010) using GEOS-5 meteorology (available at http://www.acd.ucar.edu/wrf-chem/). Photolysis rates are calculated using the FAST-J scheme (Bian and Prather, 2002). WRF-Chem is described in further detail by Grell et al. (2005).

The domain is shown in Fig. B1. We exclude results south of 53° N, over water, and over snow/ice. Additionally, we remove the first five boxes on all sides to allow for relaxation of the boundary conditions which come from the MOZART-4 model using GEOS-5 meteorology (Emmons et al., 2010). For the remainder of the grid boxes, we take a 24 h boundary layer (a median of 8 vertical levels at midday) average for the last two weeks of the run. When we bin the results by NO_x for Figs. 5 and 6 (midpoint of the bin shown by the symbols in the figures), we exclude any bin with fewer than five points in the bin. Consequently, all NO_x concentrations greater than 250 pptv are excluded.

B2 Chemical mechanism

A complete description of the WRF-Chem chemical mechanism can be found in Browne and Cohen (2012) and Browne (2012). Here we provide a brief overview of the chemical mechanism which is based on RACM2 chemistry

(Goliff and Stockwell, 2010; Stockwell et al., 2010) with substantial modifications to the $RONO_2$ and isoprene chemistry. The isoprene chemistry is based on Paulot et al. (2009a, b) and uses ozonolysis rates of isoprene-derived nitrates from Lockwood et al. (2010). The formation of a hydroperoxyaldehyde (HPALD) from the 1,6 H-shift of isoprene peroxy radicals is included using the rate constant measured by Crounse et al. (2011). Photolysis of HPALD is the same as assumed in Stavrakou et al. (2010) with the assumption that one OH is generated. Loss of HPALD also occurs through reaction with OH and is assumed to regenerate OH (Peeters and Müller, 2010). When the first generation isoprene-derived nitrates react with OH between 0 % and 65 % of the nitrogen is returned as NO_x. The exact amount of NO_x returned depends on whether the isoprene nitrate peroxy radical reacts with HO_2 (with an assumed 100 % yield of a multi-functional nitrate) or with NO or other peroxy radicals (to return between $\sim$ 34 % and $\sim$ 65 % of the nitrogen as NO_x). Ozonolysis of the first generation nitrates is assumed to return 32.7 % (for β-hydroxy isoprene nitrates) or 44.5 % (for δ-hydroxy isoprene nitrates) of the nitrogen as per MCM v3.2 (Jenkin et al., 1997; Saunders et al., 2003). Based on Geiger et al. (2003) the NO_3+ isoprene reaction forms an organic nitrate that is oxidized by OH to return 0 % of the NO_x. There are no reactions between NO_3 and the isoprene-derived nitrates in the chemical mechanism. Monoterpene derived nitrates are oxidized to form HNO_3; all other nitrates are assumed to release NO_2 with 100 % efficiency when oxidized by OH.

Photolysis of $RONO_2$ is assumed to release NO_2 with 100 % efficiency except for the photolysis of the peroxide nitrate formed from reaction of an isoprene nitrate peroxy radical with HO_2. As per MCM v3.2, we assume that photolysis results in OH and an alkoxy radical which then decomposes. We assume that $\sim 1/3$ of the alkoxy radicals will release NO_2 when they decompose. Photolysis cross-sections of $RONO_2$ were calculated using FAST-JX 6.5 (Bian and Prather, 2002) and include enhancement from carbonyl groups (Barnes et al., 1993) and reductions from hydroxy groups (Roberts and Fajer, 1989) where appropriate. Dry deposition rates of $RONO_2$ follow Ito et al. (2007) and there is no wet deposition for any species.

The monoterpene chemistry includes two lumped monoterpenes: α-pinene to represent low-reactivity monoterpenes and limonene to represent high reactivity monoterpenes. The nitrate yield from the reaction of the α-pinene peroxy radical with NO is set to 18% (similar to that measured by Nozière et al. (1998)) and is set to 22% for the limonene peroxy radical reaction (based on Leungsakul et al. (2005)). The α-pinene-derived nitrate is assumed to be a mix of both unsaturated (yield of 0.12) and saturated (yield of 0.06) nitrates while the limonene-derived nitrate is assumed to be unsaturated. Oxidation rates by OH are calculated using weighted averages of the MCM v3.2 rates for α-pinene and β-pinene (50-50 mixture) for the saturated nitrate and from limonene for the unsaturated nitrate. The ozonolysis rate of the unsaturated nitrate is calculated using the EPA Estimation Program Interface (EPI) Suite v4.1 (available at http://www.epa.gov/opptintr/exposure/pubs/episuite.htm) (US EPA, 2011). All the oxidation reactions are assumed to form a more highly functionalized nitrate that has the same chemical properties as HNO_3. The oxidation of the monoterpenes by NO_3 forms two nitrooxy-peroxy radicals. One of these primarily decomposes (formed 90% of the time for α-pinene and 29% of the time for limonene) while the other primarily reacts to form a nitrate. We assume that the nitrates formed from these reactions are split 70/30 between saturated/unsaturated nitrates.

There is no heterogeneous hydrolysis of N_2O_5 in the WRF-Chem model, however this should be a small NO_x sink under low NO_x conditions and we anticipate no significant change to the results if heterogeneous N_2O_5 hydrolysis were included.

Acknowledgements. We thank Wendy Goliff for providing the RACM2 chemical mechanism and Lukas Valin for helpful discussions regarding the WRF-Chem model. The WRF-Chem model was run on the Mako cluster supported by the UC Shared Research Computing Services and we thank the consultants for their technical help. This work was supported by a NASA Earth Systems Science Fellowship to ECB.

Edited by: P. O. Wennberg

References

Alvarado, M. J., Logan, J. A., Mao, J., Apel, E., Riemer, D., Blake, D., Cohen, R. C., Min, K.-E., Perring, A. E., Browne, E. C., Wooldridge, P. J., Diskin, G. S., Sachse, G. W., Fuelberg, H., Sessions, W. R., Harrigan, D. L., Huey, G., Liao, J., Case-Hanks, A., Jimenez, J. L., Cubison, M. J., Vay, S. A., Weinheimer, A. J., Knapp, D. J., Montzka, D. D., Flocke, F. M., Pollack, I. B., Wennberg, P. O., Kurten, A., Crounse, J., Clair, J. M. St., Wisthaler, A., Mikoviny, T., Yantosca, R. M., Carouge, C. C., and Le Sager, P.: Nitrogen oxides and PAN in plumes from boreal fires during ARCTAS-B and their impact on ozone: an integrated analysis of aircraft and satellite observations, Atmos. Chem. Phys., 10, 9739–9760, doi:10.5194/acp-10-9739-2010, 2010.

Archibald, A. T., Levine, J. G., Abraham, N. L., Cooke, M. C., Edwards, P. M., Heard, D. E., Jenkin, M. E., Karunaharan, A., Pike, R. C., Monks, P. S., Shallcross, D. E., Telford, P. J., Whalley, L. K. and Pyle, J. A.: Impacts of HO_x regeneration and recycling in the oxidation of isoprene: Consequences for the composition of past, present and future atmospheres, Geophys. Res. Lett., 38, L05804, doi:10.1029/2010GL046520, 2011.

Arey, J., Aschmann, S. M., Kwok, E. S. C. and Atkinson, R.: Alkyl nitrate, hydroxyalkyl nitrate, and hydroxycarbonyl formation from the NO_x-air photooxidations of C5-C8 n-alkanes, J. Phys. Chem. A, 105, 1020–1027, doi:10.1021/jp003292z, 2001.

Atkinson, R., Aschmann, S. M., Carter, W. P. L., Winer, A. M. and Pitts, J. N.: Alkyl nitrate formation from the nitrogen oxide (NO_x)-air photooxidations of C2-C8 n-alkanes, J. Phys. Chem., 86, 4563–4569, doi:10.1021/j100220a022, 1982.

Atkinson, R., Baulch, D. L., Cox, R. A., Crowley, J. N., Hampson, R. F., Hynes, R. G., Jenkin, M. E., Rossi, M. J., and Troe, J.: Evaluated kinetic and photochemical data for atmospheric chemistry: Volume I - gas phase reactions of O_x, HO_x, NO_x and SO_x species, Atmos. Chem. Phys., 4, 1461–1738, doi:10.5194/acp-4-1461-2004, 2004.

Atkinson, R., Baulch, D. L., Cox, R. A., Crowley, J. N., Hampson, R. F., Hynes, R. G., Jenkin, M. E., Rossi, M. J., Troe, J., and IUPAC Subcommittee: Evaluated kinetic and photochemical data for atmospheric chemistry: Volume II – gas phase reactions of organic species, Atmos. Chem. Phys., 6, 3625–4055, doi:10.5194/acp-6-3625-2006, 2006.

Barnes, I., Becker, K. H., and Zhu, T.: Near UV absorption spectra and photolysis products of difunctional organic nitrates: Possible importance as NO_x reservoirs, J. Atmos. Chem., 17, 353–373, doi:10.1007/BF00696854, 1993.

Beaver, M. R., Clair, J. M. St., Paulot, F., Spencer, K. M., Crounse, J. D., LaFranchi, B. W., Min, K. E., Pusede, S. E., Wooldridge, P. J., Schade, G. W., Park, C., Cohen, R. C., and Wennberg, P. O.: Importance of biogenic precursors to the budget of organic nitrates: observations of multifunctional organic nitrates by CIMS and TD-LIF during BEARPEX 2009, Atmos. Chem. Phys., 12, 5773–5785, doi:10.5194/acp-12-5773-2012, 2012.

Bertram, T. H., Heckel, A., Richter, A., Burrows, J. P., and Cohen, R. C.: Satellite measurements of daily variations in soil NO_x emissions, Geophys. Res. Lett., 32, L24812, doi:10.1029/2005GL024640, 2005.

Bian, H. and Prather, M. J.: Fast-J2: Accurate Simulation of Stratospheric Photolysis in Global Chemical Models, J. Atmos. Chem., 41, 281–296, doi:10.1023/A:1014980619462, 2002.

Bonan, G. B. and Levis, S.: Quantifying carbon-nitrogen feedbacks in the Community Land Model (CLM4), Geophys. Res. Lett., 37, L07401, doi:10.1029/2010GL042430, 2010.

Brown, S. S., deGouw, J. A., Warneke, C., Ryerson, T. B., Dubé, W. P., Atlas, E., Weber, R. J., Peltier, R. E., Neuman, J. A., Roberts, J. M., Swanson, A., Flocke, F., McKeen, S. A., Brioude, J., Sommariva, R., Trainer, M., Fehsenfeld, F. C. and Ravishankara, A. R.: Nocturnal isoprene oxidation over the Northeast United States in summer and its impact on reactive nitrogen partitioning and secondary organic aerosol, Atmos. Chem. Phys., 9, 3027–3042, doi:10.5194/acp-9-3027-2009, 2009.

Browne, E. C.: Observational constraints on the photochemistry of non-acyl peroxy nitrates and organic nitrates on regional and global scales, Ph.D. dissertation, University of California, Berkeley, U.S.A., 2012.

Browne, E. C. and Cohen, R. C.: Impacts of monoterpene nitrates on NO_x and NO_y in the Boreal, forest, Atmos. Chem. Phys. Discuss., in preparation, 2012.

Browne, E. C., Min, K.-E., Wooldridge, P. J., Apel, E., Blake, D. R., Cantrell, C. A., Cubison, M. J., Jimenez, J. L., Weinheimer, A. J., Wennberg, P. O., Wisthaler, A., and Cohen, R. C.: Observations of total $RONO_2$ over the Boreal forest: NO_x sinks and HNO_3 sources, Atmos. Chem. Phys. Discuss., submitted, 2012.

Carlton, A. G., Pinder, R. W., Bhave, P. V., and Pouliot, G. A.: To what extent can biogenic SOA be controlled?, Environ. Sci. Tech., 44, 3376–3380, doi:10.1021/es903506b, 2010.

Cleary, P. A., Murphy, J. G., Wooldridge, P. J., Day, D. A., Millet, D. B., McKay, M., Goldstein, A. H., and Cohen, R. C.: Observations of total alkyl nitrates within the Sacramento Urban Plume, Atmos. Chem. Phys. Discuss., 5, 4801–4843, doi:10.5194/acpd-5-4801-2005, 2005.

Crounse, J. D., Knap, H. C., Ørnsø, K. B., Jørgensen, S., Paulot, F., Kjaergaard, H. G., and Wennberg, P. O.: Atmospheric fate of methacrolein. 1. Peroxy radical isomerization following addition of OH and O_2, J. Phys. Chem. A, 116, 5756–5762, doi:10.1021/jp211560u, 2012.

Crounse, J. D., Paulot, F., Kjaergaard, H. G., and Wennberg, P. O.: Peroxy radical isomerization in the oxidation of isoprene, Phys. Chem. Chem. Phys., 13, 13607, doi:10.1039/c1cp21330j, 2011.

Dallmann, T. R. and Harley, R. A.: Evaluation of mobile source emission trends in the United States, J. Geophys. Res., 115, D14305, doi:10.1029/2010JD013862, 2010.

Day, D. A., Farmer, D. K., Goldstein, A. H., Wooldridge, P. J., Minejima, C., and Cohen, R. C.: Observations of NO_x, ΣPNs, ΣANs, and HNO_3 at a Rural Site in the California Sierra Nevada Mountains: summertime diurnal cycles, Atmos. Chem. Phys., 9, 4879–4896, doi:10.5194/acp-9-4879-2009, 2009.

Day, D. A., Wooldridge, P. J., Dillon, M. B., Thornton, J. A., and Cohen, R. C.: A thermal dissociation laser-induced fluorescence instrument for in situ detection of NO_2, peroxy nitrates, alkyl nitrates, and HNO_3, J. Geophys. Res., 107, 4046, doi:10.1029/2001JD000779, 2002.

Derwent, R., Stevenson, D., Doherty, R., Collins, W., Sanderson, M., and Johnson, C.: Radiative forcing from surface NO_x emissions: spatial and seasonal variations, Climatic Change, 88, 385–401, doi:10.1007/s10584-007-9383-8, 2008.

Emmons, L. K., Walters, S., Hess, P. G., Lamarque, J.-F., Pfister, G. G., Fillmore, D., Granier, C., Guenther, A., Kinnison, D., Laepple, T., Orlando, J., Tie, X., Tyndall, G., Wiedinmyer, C., Baughcum, S. L., and Kloster, S.: Description and evaluation of the Model for Ozone and Related chemical Tracers, version 4 (MOZART-4), Geosci. Model Dev., 3, 43–67, doi:10.5194/gmd-3-43-2010, 2010.

Farmer, D. K. and Cohen, R. C.: Observations of HNO_3, ΣAN, ΣPN and NO_2 fluxes: evidence for rapid HO_x chemistry within a pine forest canopy, Atmos. Chem. Phys., 8, 3899–3917, doi:10.5194/acp-8-3899-2008, 2008.

Farmer, D. K., Perring, A. E., Wooldridge, P. J., Blake, D. R., Baker, A., Meinardi, S., Huey, L. G., Tanner, D., Vargas, O., and Cohen, R. C.: Impact of organic nitrates on urban ozone production, Atmos. Chem. Phys., 11, 4085–4094, doi:10.5194/acp-11-4085-2011, 2011.

Fiore, A. M., Horowitz, L. W., Purves, D. W., II, H. L., Evans, M. J., Wang, Y., Li, Q., and Yantosca, R. M.: Evaluating the contribution of changes in isoprene emissions to surface ozone trends over the eastern United States, J. Geophys. Res., 110, D12303, doi:10.1029/2004JD005485, 2005.

Freitas, S. R., Longo, K. M., Alonso, M. F., Pirre, M., Marecal, V., Grell, G., Stockler, R., Mello, R. F., and Sánchez Gácita, M.: PREP-CHEM-SRC – 1.0: a preprocessor of trace gas and aerosol emission fields for regional and global atmospheric chemistry models, Geosci. Model Dev., 4, 419–433, doi:10.5194/gmd-4-419-2011, 2011.

Fry, J. L., Kiendler-Scharr, A., Rollins, A. W., Brauers, T., Brown, S. S., Dorn, H.-P., Dubé, W. P., Fuchs, H., Mensah, A., Rohrer, F., Tillmann, R., Wahner, A., Wooldridge, P. J., and Cohen, R. C.: SOA from limonene: role of NO_3 in its generation and degradation, Atmos. Chem. Phys., 11, 3879–3894, doi:10.5194/acp-11-

3879-2011, 2011.

Fry, J. L., Kiendler-Scharr, A., Rollins, A. W., Wooldridge, P. J., Brown, S. S., Fuchs, H., Dubé, W., Mensah, A., dal Maso, M., Tillmann, R., Dorn, H.-P., Brauers, T., and Cohen, R. C.: Organic nitrate and secondary organic aerosol yield from NO_3 oxidation of β-pinene evaluated using a gas-phase kinetics/aerosol partitioning model, Atmos. Chem. Phys., 9, 1431–1449, doi:10.5194/acp-9-1431-2009, 2009.

Fry, M. M., Naik, V., West, J. J., Schwarzkopf, M. D., Fiore, A. M., Collins, W. J., Dentener, F. J., Shindell, D. T., Atherton, C., Bergmann, D., Duncan, B. N., Hess, P., MacKenzie, I. A., Marmer, E., Schultz, M. G., Szopa, S., Wild, O., and Zeng, G.: The influence of ozone precursor emissions from four world regions on tropospheric composition and radiative climate forcing, J. Geophys. Res., 117, D07306, doi:10.1029/2011JD017134, 2012.

Fuglestvedt, J. S., Berntsen, T. K., Isaksen, I. S. A., Mao, H. T., Liang, X. Z., and Wang, W. C.: Climatic forcing of nitrogen oxides through changes in tropospheric ozone and methane; global 3D model studies, Atmos. Environ., 33, 961–977, doi:10.1016/S1352-2310(98)00217-9, 1999.

Galloway, J. N., Townsend, A. R., Erisman, J. W., Bekunda, M., Cai, Z., Freney, J. R., Martinelli, L. A., Seitzinger, S. P., and Sutton, M. A.: Transformation of the Nitrogen cycle: Recent trends, questions, and potential solutions, Science, 320, 889–892, doi:10.1126/science.1136674, 2008.

Geiger, H., Barnes, I., Bejan, J., Benter, T., and Spittler, M.: The tropospheric degradation of isoprene: an updated module for the regional atmospheric chemistry mechanism, Atmos. Environ., 37, 1503–1519, doi:10.1016/S1352-2310(02)01047-6, 2003.

Ghude, S. D., Lal, D. M., Beig, G., A, R. van der and Sable, D.: Rain-induced soil NO_x emission from India during the onset of the summer monsoon: A satellite perspective, J. Geophys. Res., 115, D16304, doi:10.1029/2009JD013367, 2010.

Goliff, W. and Stockwell, W. R.: The Regional Atmospheric Chemistry Mechanism, Version 2 – a final frozen version at last, Atmospheric Chemical Mechanisms Conference, Davis, CA, USA, 2010.

Grell, G. A., Peckham, S. E., Schmitz, R., McKeen, S. A., Frost, G., Skamarock, W. C., and Eder, B.: Fully coupled "online" chemistry within the WRF model, Atmos. Environ., 39, 6957–6975, doi:10.1016/j.atmosenv.2005.04.027, 2005.

Guenther, A., Karl, T., Harley, P., Wiedinmyer, C., Palmer, P. I., and Geron, C.: Estimates of global terrestrial isoprene emissions using MEGAN (Model of Emissions of Gases and Aerosols from Nature), Atmos. Chem. Phys., 6, 3181–3210, doi:10.5194/acp-6-3181-2006, 2006.

Henderson, B. H., Pinder, R. W., Crooks, J., Cohen, R. C., Carlton, A. G., Pye, H. O. T., and Vizuete, W.: Combining Bayesian methods and aircraft observations to constrain the $HO^{\bullet}$ + NO_2 reaction rate, Atmos. Chem. Phys., 12, 653–667, doi:10.5194/acp-12-653-2012, 2012.

Holland, E. A., Braswell, B. H., Lamarque, J.-F., Townsend, A., Sulzman, J., Müller, J.-F., Dentener, F., Brasseur II, G.,, H. L., Penner, J. E., and Roelofs, G.-J.: Variations in the predicted spatial distribution of atmospheric nitrogen deposition and their impact on carbon uptake by terrestrial ecosystems, J. Geophys. Res., 102, 15849–15866, doi:10.1029/96JD03164, 1997.

Horowitz, L. W., Fiore, A. M., Milly, G. P., Cohen, R. C., Perring, A., Wooldridge, P. J., Hess, P. G., Emmons, L. K., and Lamarque, J.-F.: Observational constraints on the chemistry of isoprene nitrates over the eastern United States, J. Geophys. Res., 112, D12S08, doi:10.1029/2006JD007747, 2007.

Horowitz, L. W., Liang, J., Gardner, G. M., and Jacob, D. J.: Export of reactive nitrogen from North America during summertime: Sensitivity to hydrocarbon chemistry, J. Geophys. Res., 103, 13451–13476, doi:10.1029/97JD03142, 1998.

Hudman, R. C., Jacob, D. J., Turquety, S., Leibensperger, E. M., Murray, L. T., Wu, S., Gilliland, A. B., Avery, M., Bertram, T. H., Brune, W., Cohen, R. C., Dibb, J. E., Flocke, F. M., Fried, A., Holloway, J., Neuman, J. A., Orville, R., Perring, A., Ren, X., Sachse, G. W., Singh, H. B., Swanson, A., and Wooldridge, P. J.: Surface and lightning sources of nitrogen oxides over the United States: Magnitudes, chemical evolution, and outflow, J. Geophys. Res., 112, D12S05, doi:10.1029/2006JD007912, 2007.

Hudman, R. C., Russell, A. R., Valin, L. C., and Cohen, R. C.: Interannual variability in soil nitric oxide emissions over the United States as viewed from space, Atmos. Chem. Phys., 10, 9943–9952, doi:10.5194/acp-10-9943-2010, 2010.

Ito, A., Sillman, S., and Penner, J. E.: Effects of additional nonmethane volatile organic compounds, organic nitrates, and direct emissions of oxygenated organic species on global tropospheric chemistry, J. Geophys. Res., 112, D06309, doi:10.1029/2005JD006556, 2007.

Ito, A., Sillman, S., and Penner, J. E.: Global chemical transport model study of ozone response to changes in chemical kinetics and biogenic volatile organic compounds emissions due to increasing temperatures: Sensitivities to isoprene nitrate chemistry and grid resolution, J. Geophys. Res., 114, D09301, doi:10.1029/2008JD011254, 2009.

Jacob, D. J., Crawford, J. H., Maring, H., Clarke, A. D., Dibb, J. E., Emmons, L. K., Ferrare, R. A., Hostetler, C. A., Russell, P. B., Singh, H. B., Thompson, A. M., Shaw, G. E., McCauley, E., Pederson, J. R., and Fisher, J. A.: The Arctic Research of the Composition of the Troposphere from Aircraft and Satellites (ARCTAS) mission: design, execution, and first results, Atmos. Chem. Phys., 10, 5191–5212, doi:10.5194/acp-10-5191-2010, 2010.

Jaeglé, L., Steinberger, L., Martin, R. V. and Chance, K.: Global partitioning of NO_x sources using satellite observations: Relative roles of fossil fuel combustion, biomass burning and soil emissions, Faraday Discuss., 130, 407–423, doi:10.1039/b502128f, 2005.

Jenkin, M. E., Saunders, S. M., and Pilling, M. J.: The tropospheric degradation of volatile organic compounds: a protocol for mechanism development, Atmos. Environ., 31, 81–104, doi:10.1016/S1352-2310(96)00105-7, 1997.

Lelieveld, J., Butler, T. M., Crowley, J. N., Dillon, T. J., Fischer, H., Ganzeveld, L., Harder, H., Lawrence, M. G., Martinez, M., Taraborrelli, D., and Williams, J.: Atmospheric oxidation capacity sustained by a tropical forest, Nature, 452, 737–740, doi:10.1038/nature06870, 2008.

Leungsakul, S., Jeffries, H. E. and Kamens, R. M.: A kinetic mechanism for predicting secondary aerosol formation from the reactions of d-limonene in the presence of oxides of nitrogen and natural sunlight, Atmos. Environ., 39, 7063—7082, doi:10.1016/j.atmosenv.2005.08.024, 2005.

Lockwood, A. L., Filley, T. R., Rhodes, D., and Shepson, P. B.: Foliar uptake of atmospheric organic nitrates, Geophys. Res. Lett., 35, L15809, doi:10.1029/2008GL034714, 2008.

Lockwood, A. L., Shepson, P. B., Fiddler, M. N., and Alaghmand, M.: Isoprene nitrates: preparation, separation, identification, yields, and atmospheric chemistry, Atmos. Chem. Phys., 10, 6169–6178, doi:10.5194/acp-10-6169-2010, 2010.

Mao, J., Ren, X., Brune, W. H., Van Duin, D. M., Cohen, R. C., Park, J.-H., Goldstein, A. H., Paulot, F., Beaver, M. R., Crounse, J. D., Wennberg, P. O., DiGangi, J. P., Henry, S. B., Keutsch, F. N., Park, C., Schade, G. W., Wolfe, G. M., and Thornton, J. A.: Insights into hydroxyl measurements and atmospheric oxidation in a California forest, Atmos. Chem. Phys. Discuss., 12, 6715–6744, doi:10.5194/acpd-12-6715-2012, 2012.

Mebust, A. K., Russell, A. R., Hudman, R. C., Valin, L. C., and Cohen, R. C.: Characterization of wildfire NO_x emissions using MODIS fire radiative power and OMI tropospheric NO_2 columns, Atmos. Chem. Phys., 11, 5839–5851, doi:10.5194/acp-11-5839-2011, 2011.

Mickley, L. J., Jacob, D. J., and Rind, D.: Uncertainty in preindustrial abundance of tropospheric ozone: Implications for radiative forcing calculations, J. Geophys. Res., 106, 3389–3399, 2001.

Murphy, J. G., Day, D. A., Cleary, P. A., Wooldridge, P. J., and Cohen, R. C.: Observations of the diurnal and seasonal trends in nitrogen oxides in the western Sierra Nevada, Atmos. Chem. Phys., 6, 5321–5338, doi:10.5194/acp-6-5321-2006, 2006.

Novelli, P. C., Lang, P. M., Masarie, K. A., Hurst, D. F., Myers, R. and Elkins, J. W.: Molecular hydrogen in the troposphere: Global distribution and budget, J. Geophys. Res.-Atmos., 104, 30427–30444, doi:10.1029/1999JD900788, 1999.

Nozière, B., Barnes, I. and Becker, K.-H.: Product study and mechanisms of the reactions of α-pinene and of pinonaldehyde with OH radicals, J. Geophys. Res., 104, 23645-–23656,doi:10.1029/1999JD900778, 1999.

Parrish, D. D., Aikin, K. C., Oltmans, S. J., Johnson, B. J., Ives, M., and Sweeny, C.: Impact of transported background ozone inflow on summertime air quality in a California ozone exceedance area, Atmos. Chem. Phys., 10, 10093–10108, doi:10.5194/acp-10-10093-2010, 2010.

Paulot, F., Crounse, J. D., Kjaergaard, H. G., Kroll, J. H., Seinfeld, J. H., and Wennberg, P. O.: Isoprene photooxidation: new insights into the production of acids and organic nitrates, Atmos. Chem. Phys., 9, 1479–1501, doi:10.5194/acp-9-1479-2009, 2009a.

Paulot, F., Crounse, J. D., Kjaergaard, H. G., Kürten, A., Clair, S., M, J., Seinfeld, J. H., and Wennberg, P. O.: Unexpected Epoxide Formation in the Gas-Phase Photooxidation of Isoprene, Science, 325, 730–733, doi:10.1126/science.1172910, 2009b.

Paulot, F., Henze, D. K., and Wennberg, P. O.: Impact of the isoprene photochemical cascade on tropical ozone, Atmos. Chem. Phys., 12, 1307–1325, doi:10.5194/acp-12-1307-2012, 2012.

Peeters, J. and Müller, J.-F.: HO_x radical regeneration in isoprene oxidation via peroxy radical isomerisations. II: experimental evidence and global impact, Phys. Chem. Chem. Phys., 12, 14227, doi:10.1039/c0cp00811g, 2010.

Peeters, J., Nguyen, T. L., and Vereecken, L.: HO_x radical regeneration in the oxidation of isoprene, Phys. Chem. Chem. Phys., 11, 5935, doi:10.1039/b908511d, 2009.

Perring, A. E., Bertram, T. H., Farmer, D. K., Wooldridge, P. J., Dibb, J., Blake, N. J., Blake, D. R., Singh, H. B., Fuelberg, H., Diskin, G., Sachse, G., and Cohen, R. C.: The production and persistence of $\Sigma RONO_2$ in the Mexico City plume, Atmos. Chem. Phys., 10, 7215–7229, doi:10.5194/acp-10-7215-2010, 2010.

Perring, A. E., Bertram, T. H., Wooldridge, P. J., Fried, A., Heikes, B. G., Dibb, J., Crounse, J. D., Wennberg, P. O., Blake, N. J., Blake, D. R., Brune, W. H., Singh, H. B., and Cohen, R. C.: Airborne observations of total $RONO_2$: new constraints on the yield and lifetime of isoprene nitrates, Atmos. Chem. Phys., 9, 1451–1463, doi:10.5194/acp-9-1451-2009, 2009a.

Perring, A. E., Pusede, S. E., and Cohen, R. C.: An observational perspective on the atmospheric impacts of alkyl and multifunctional nitrates on ozone and secondary organic aerosol, Chem. Rev., in preparation, 2012.

Perring, A. E., Wisthaler, A., Graus, M., Wooldridge, P. J., Lockwood, A. L., Mielke, L. H., Shepson, P. B., Hansel, A., and Cohen, R. C.: A product study of the isoprene+NO_3 reaction, Atmos. Chem. Phys., 9, 4945–4956, doi:10.5194/acp-9-4945-2009, 2009b.

Pinder, R. W., Davidson, E. A., Goodale, C. L., Greaver, T. L., Herrick, J. D., and Liu, L.: Climate change impacts of US reactive nitrogen, P. Natl. Acad. Sci. USA, 109, 7671–7675, doi:10.1073/pnas.1114243109, 2012.

Pye, H. O. T., Chan, A. W. H., Barkley, M. P., and Seinfeld, J. H.,: Global modeling of organic aerosol: the importance of reactive nitrogen (NO_x and NO_3), Atmos. Chem. Phys., 10, 11261–11276, doi:10.5194/acp-10-11261-2010, 2010.

Roberts, J. M. and Fajer, R. W.: UV absorption cross sections of organic nitrates of potential atmospheric importance and estimation of atmospheric lifetimes, Environ. Sci. Technol., 23, 945–951, doi:10.1021/es00066a003, 1989.

Rollins, A. W., Kiendler-Scharr, A., Fry, J. L., Brauers, T., Brown, S. S., Dorn, H.-P., Dubé, W. P., Fuchs, H., Mensah, A., Mentel, T. F., Rohrer, F., Tillmann, R., Wegener, R., Wooldridge, P. J., and Cohen, R. C.: Isoprene oxidation by nitrate radical: alkyl nitrate and secondary organic aerosol yields, Atmos. Chem. Phys., 9, 6685–6703, doi:10.5194/acp-9-6685-2009, 2009.

Rollins, A. W., Browne, E. C., Min, K.-E., Pusede, S. E., Wooldridge, P. J., Gentner, D. R., Goldstein, A. H., Liu, S., Day, D. A., Russell, L. M. and Cohen, R. C.: Evidence for NO_x control over nighttime SOA formation, Science, 337, 1210-–1212, doi:10.1126/science.1221520, 2012.

Rosen, R. S., Wood, E. C., Wooldridge, P. J., Thornton, J. A., Day, D. A., Kuster, W., Williams, E. J., Jobson, B. T., and Cohen, R. C.: Observations of total alkyl nitrates during Texas Air Quality Study 2000: Implications for O_3 and alkyl nitrate photochemistry, J. Geophys. Res., 109, D07303, doi:10.1029/2003JD004227, 2004.

Russell, A. R., Valin, L. C., Bucsela, E. J., Wenig, M. O., and Cohen, R. C.: Space-based constraints on spatial and temporal patterns of NO_x emissions in California, 2005–2008, Environ. Sci. Technol., 44, 3608–3615, doi:10.1021/es903451j, 2010.

Russell, A. R., Valin, L. C., and Cohen, R. C.: Trends in OMI NO_2 observations over the US: effects of emission control technology and the economic recession, Atmos. Chem. Phys. Discuss., 12, 15419–15452, doi:10.5194/acpd-12-15419-2012, 2012.

Sander, S. P., Abbatt, J., Barker, J. R., Burkholder, J. B., Friedl, R. R., Golden, D. M., Huie, R. E., Kolb, C. E., Kurylo, M. J., Moortgat, G. K., Orkin, V. L., and Wine, P. H.: Chemical kinet-

ics and photochemical data for use in atmospheric studies, Evaluation No. 17, JPL Publication 10-6, Jet Propulsion Laboratory, Pasadena, 2011, http://jpldataeval.jpl.nasa.gov, 2011.

Saunders, S. M., Jenkin, M. E., Derwent, R. G., and Pilling, M. J.: Protocol for the development of the Master Chemical Mechanism, MCM v3 (Part A): tropospheric degradation of non-aromatic volatile organic compounds, Atmos. Chem. Phys., 3, 161–180, doi:10.5194/acp-3-161-2003, 2003.

Schumann, U. and Huntrieser, H.: The global lightning-induced nitrogen oxides source, Atmos. Chem. Phys., 7, 3823–3907, doi:10.5194/acp-7-3823-2007, 2007.

Sillman, S. and Samson, P. J.: Impact of temperature on oxidant photochemistry in urban, polluted rural and remote environments, J. Geophys. Res., 100, 11497–11508, doi:10.1029/94JD02146, 1995.

St. Clair, J. M., McCabe, D. C., Crounse, J. D., Steiner, U., and Wennberg, P. O.: Chemical ionization tandem mass spectrometer for the in situ measurement of methyl hydrogen peroxide, Rev. Sci. Instrum., 81, 094102, doi:10.1063/1.3480552, 2010.

Stavrakou, T., Peeters, J., and Müller, J.-F.: Improved global modelling of HO_x recycling in isoprene oxidation: evaluation against the GABRIEL and INTEX-A aircraft campaign measurements, Atmos. Chem. Phys., 10, 9863–9878, doi:10.5194/acp-10-9863-2010, 2010.

Stockwell, W. R., Goliff, W. S., and Lawson, C. V.: RACM Developments, Atmospheric Chemical Mechanisms Conference, Davis, CA, USA, 2010.

Stone, D., Evans, M. J., Edwards, P. M., Commane, R., Ingham, T., Rickard, A. R., Brookes, D. M., Hopkins, J., Leigh, R. J., Lewis, A. C., Monks, P. S., Oram, D., Reeves, C. E., Stewart, D., and Heard, D. E.: Isoprene oxidation mechanisms: measurements and modelling of OH and HO_2 over a South-East Asian tropical rainforest during the OP3 field campaign, Atmos. Chem. Phys., 11, 6749–6771, doi:10.5194/acp-11-6749-2011, 2011.

Taraborrelli, D., Lawrence, M. G., Crowley, J. N., Dillon, T. J., Gromov, S., Groß, C. B. M., Vereecken, L., and Lelieveld, J.: Hydroxyl radical buffered by isoprene oxidation over tropical forests, Nature Geosci., 5, 190–193, doi:10.1038/ngeo1405, 2012.

Thornberry, T., Carroll, M. A., Keeler, G. J., Sillman, S., Bertman, S. B., Pippin, M. R., Ostling, K., Grossenbacher, J. W., Shepson, P. B., Cooper, O. R., Moody, J. L., and Stockwell, W. R.: Observations of reactive oxidized nitrogen and speciation of NO_y during the PROPHET summer 1998 intensive, J. Geophys. Res., 106, 24359–24386, doi:10.1029/2000JD900760, 2001.

Thornton, P. E., Doney, S. C., Lindsay, K., Moore, J. K., Mahowald, N., Randerson, J. T., Fung, I., Lamarque, J.-F., Feddema, J. J., and Lee, Y.-H.: Carbon-nitrogen interactions regulate climate-carbon cycle feedbacks: results from an atmosphere-ocean general circulation model, Biogeosciences, 6, 2099–2120, doi:10.5194/bg-6-2099-2009, 2009.

Thornton, P. E., Lamarque, J.-F., Rosenbloom, N. A., and Mahowald, N. M.: Influence of carbon-nitrogen cycle coupling on land model response to CO_2 fertilization and climate variability, Global Biogeochem. Cy., 21, GB4018, doi:10.1029/2006GB002868, 2007.

Trainer, M., Buhr, M. P., Curran, C. M., Fehsenfeld, F. C., Hsie, E. Y., Liu, S. C., Norton, R. B., Parrish, D. D., Williams, E. J., Gandrud, B. W., Ridley, B. A., Shetter, J. D., Allwine, E. J., and Westberg, H. H.: Observations and modeling of the reactive nitrogen photochemistry at a rural site, J. Geophys. Res., 96, 3045–3063, doi:10.1029/90JD02395, 1991.

US EPA: Estimation programs interface Suite for Microsoft Windows v4.1, 2011.

Valin, L. C., Russell, A. R., Hudman, R. C., and Cohen, R. C.: Effects of model resolution on the interpretation of satellite NO_2 observations, Atmos. Chem. Phys., 11, 11647–11655, doi:10.5194/acp-11-11647-2011, 2011.

van der A, R. J., Eskes, H. J., Boersma, K. F., Noije, T. P. C. van, Roozendael, M. V., Smedt, I. D., Peters, D. H. M. U., and Meijer, E. W.: Trends, seasonal variability and dominant NO_x source derived from a ten year record of NO_2 measured from space, J. Geophys. Res., 113, D04302, doi:10.1029/2007JD009021, 2008.

von Kuhlmann, R., Lawrence, M. G., Pöschl, U., and Crutzen, P. J.: Sensitivities in global scale modeling of isoprene, Atmos. Chem. Phys., 4, 1–17, doi:10.5194/acp-4-1-2004, 2004.

Whalley, L. K., Edwards, P. M., Furneaux, K. L., Goddard, A., Ingham, T., Evans, M. J., Stone, D., Hopkins, J. R., Jones, C. E., Karunaharan, A., Lee, J. D., Lewis, A. C., Monks, P. S., Moller, S. J., and Heard, D. E.: Quantifying the magnitude of a missing hydroxyl radical source in a tropical rainforest, Atmos. Chem. Phys., 11, 7223–7233, doi:10.5194/acp-11-7223-2011, 2011.

Wiedinmyer, C., Quayle, B., Geron, C., Belote, A., McKenzie, D., Zhang, X., O'Neill, S., and Wynne, K. K.: Estimating emissions from fires in North America for air quality modeling, Atmos. Environ., 40, 3419–3432, doi:10.1016/j.atmosenv.2006.02.010, 2006.

Wild, O., Prather, M. J., and Akimoto, H.: Indirect long-term global radiative cooling from NO_x emissions, Geophys. Res. Lett., 28, 1719–1722, doi:10.1029/2000GL012573, 2001.

Wu, S., Mickley, L. J., Jacob, D. J., Logan, J. A., Yantosca, R. M., and Rind, D.: Why are there large differences between models in global budgets of tropospheric ozone?, J. Geophys. Res., 112, D05302, doi:10.1029/2006JD007801, 2007.

Zhang, L., Jacob, D. J., Boersma, K. F., Jaffe, D. A., Olson, J. R., Bowman, K. W., Worden, J. R., Thompson, A. M., Avery, M. A., Cohen, R. C., Dibb, J. E., Flock, F. M., Fuelberg, H. E., Huey, L. G., McMillan, W. W., Singh, H. B., and Weinheimer, A. J.: Transpacific transport of ozone pollution and the effect of recent Asian emission increases on air quality in North America: an integrated analysis using satellite, aircraft, ozonoesond, and surface observations, Atmos. Chem. Phys., 8, 6117–6136, doi:10.5194/acp-8-6117-2008, 2008.